

FERRITE ROTARY-FIELD PHASE SHIFTERS WITH REDUCED CROSS-SECTION

C.R. Boyd, Jr. and C.M. Oness
Microwave Applications Group
Santa Maria, California

ABSTRACT

Practical ferrite Rotary-Field phase shifters can be built for the 1.3 GHz. frequency region by using a reduced-diameter circular waveguide in which disks of high dielectric constant material and ferrite-filled sections alternate. This approach permits reduction of the guide diameter to about half that needed for uniform filling with garnet material only.

Experimental results for feasibility-study units at 2.5 GHz. and 1.3 GHz. confirm that the reduced-diameter configuration can produce high phase setting accuracy, but with increased insertion loss.

INTRODUCTION

Ferrite Rotary-Field phase shifters⁽¹⁾ can be built to provide superior phase setting accuracy at high power levels over bandwidths up to about fifteen percent. Designs currently exist for operation at center frequencies from roughly 3 GHz. to 20 GHz. Extension of the design approach to lower frequencies, e.g. in the 1-2 GHz. range, is difficult because of the large diameter of ferrite rod required. For example, a conventional Rotary-Field phase shifter design for use at a center frequency of 1.3 GHz. would require a ferrite rod with a diameter on the order of 2.4 inches (6.1 cm.).

This paper describes a technique for reducing the diameter of a Rotary-Field phase shifter by the use of a waveguide loaded with disks of high dielectric constant material. In this approach the circular waveguide uniformly filled with ferrite is replaced by a filter-like structure in which dielectric and ferrite filled sections alternate, in a geometry of approximately half the diameter of the uniformly filled case.

Although the longitudinal variation of the fields in the unmagnetized ferrite is described by hyperbolic rather than trigonometric functions, theory^(2,3) predicts that transverse-field magnetic bias will produce birefringence-type differential phase. Data measured on phase shifters operating at 2.5 GHz. and 1.3 GHz. confirm this prediction.

The material presented below describes the basic configuration, discusses briefly the design approach, and shows measured results on the two feasibility models fabricated.

BASIC CONFIGURATION

Figure 1 shows an exploded view of the L-Band composite rod design approach. In this diagram, the alternating dielectric-ferrite sections are clearly evident, along with typical dielectric quarter-wave plates and transformers for matching into coaxial line at each end of the structure. The S-Band unit design was similar, but matched into rectangular waveguide at both ends. The transformers incorporate the usual film load feature for damping cross-polarized error waves at each end. The bias yoke has the same form as for an ordinary Rotary-Field phase shifter, providing an electrically rotatable fourpole transverse magnetic field in the ferrite. Because the ferrite-dielectric segment boundaries are also transverse, no angle-dependent bias field distortion occurs.

Figure 2 shows the computed pass-band impedance match characteristic of the composite rod waveguide for the S-Band feasibility model; obviously, the response is much broader than needed, indicating that a smaller number of thicker sections could have sufficed.

DESIGN CONSIDERATIONS

The aggregate length of ferrite is determined by the same method⁽²⁾ as in the uniformly filled case. That is, the differential phase $\Delta\phi$ between normal modes is taken as,

$$\Delta\phi \equiv 260.2 \frac{l_p}{d} \frac{\kappa}{\mu} \quad (1)$$

where l_p is the total ferrite length, d is the guide diameter, μ and κ are magnitudes of the diagonal and off-diagonal terms of the permeability tensor transverse to the bias field direction. The values of μ and κ are determined differently under "weak bias" and "strong bias" conditions. For the "weak bias" case⁽⁴⁾,

$$\mu \approx \mu_i + (1-\mu_i) \frac{\tanh(1.25 \frac{M}{M_s})}{\tanh(1.25)} \quad (2)$$

$$\kappa \approx \frac{M}{M_s} \frac{\omega M}{\omega} \quad (3)$$

with the initial permeability μ_i given by

$$\mu_i = \frac{1}{3} + \frac{2}{3} \sqrt{1 - \left(\frac{\omega_M}{\omega}\right)^2} \quad (4)$$

For the "strong bias" case,

$$\mu = 1 + \frac{\omega_0 \omega_M}{\omega_0^2 - \omega^2} \quad (5)$$

$$\kappa = \frac{M}{M_s} \left(\frac{\omega \omega_M}{\omega_0^2 - \omega^2} \right) \quad (6)$$

with ω_0 given by

$$\omega_0 = \omega_M \sqrt{\frac{M}{M_s} \left(\frac{M}{M_s} - \frac{1}{2} \right)} \quad (7)$$

In equations (2) through (7), M_s is the saturation magnetic moment of the ferrite, M/M_s is the bias level, ω is the operating frequency, and ω_M is the material characteristic frequency equal to the product of the gyromagnetic ratio and the saturation moment. For practical design purposes, it has been found empirically that for typical low-coercive-force materials, the "weak-bias" case can be used up to $M/M_s \approx 0.6$, while the "strong-bias" case should be used above $M/M_s \approx 1.0$. In the transition region, values linearly interpolated between the two cases have been used successfully in approximating κ and μ .

Design of the dielectric quarter-wave plates proceeds in the usual manner, with a centered slab of higher dielectric constant material extending along the waveguide axis, and with quarter-wave transformer matching sections at each end. Compared with uniformly filled designs, however, the values of relative dielectric constant are much higher. Both the composite ferrite-dielectric rod assembly and the quarter-wave plates were designed to provide a good impedance match into circular waveguide uniformly filled with material of relative dielectric constant $\epsilon_r = 30$.

MEASURED RESULTS

Figure 3 shows a hysteresis-loop characteristic of differential phase versus current, measured at 1.3 GHz. on the L-Band model. For this measurement, the quarter-wave plates were rotated 45 degrees so that propagation through the structure involved linear polarization only. Frequency dependence of the measured maximum differential phase is compared in Figure 4 with theoretical values based on a

300 Gauss material operating at a bias level $M/M_s = 0.81$. The phase values are much higher than the required 180 degrees because the unit was designed for operation at $M/M_s = 0.6$. Similar characteristics were observed on the S-Band unit, which also had a conservatively designed half-wave plate section.

Figures 5, 6, and 7 give insertion loss, return loss, and phase accuracy plots for the S-Band design. In the first two plots, the envelope of all values was made by scanning through the entire phase shift range while slowly sweeping frequency. The phase error plot indicates about ± 1 degree accuracy, with a hysteresis level of about 8 degrees, i.e. the offset between continuously increasing and continuously decreasing command angle values. Finally, Figure 8 presents preliminary insertion loss and return loss data for the L-Band model. At the early stage of development shown, it is clear that the impedance match needs to be improved; however, the insertion loss data are very encouraging.

CONCLUSIONS

A technique has been described by which the high accuracy, high power handling possibilities offered by the ferrite Rotary-Field phase shifter can be extended to low microwave frequencies in a structure that is practical to build. Good correspondence between measured data and approximate theory have been obtained for the ferrite rotatable half-wave plate.

REFERENCES

- (1) C. R. Boyd, Jr., "An accurate analog ferrite phaser," 1971 G-MTT International Symposium Digest, pp. 104-105, May 1971.
- (2) C. R. Boyd, Jr., "Design of ferrite differential phaser sections," 1975 S-MTT International Symposium Digest, pp. 240-242, May 1975.
- (3) C. R. Boyd, Jr., "A transmission line model for the lossless ferrite-loaded non-reciprocal waveguide," 1985 International Symposium of Microwave Technology in Industrial Development, Brazil, pp. 209-216, July 1985.
- (4) J. J. Green, C.E. Patton, and F. Sandy, "Microwave properties of partially magnetized ferrite," Rome Air Development Center, Rome, NY, Final Report RADC-TR-68-312, August 1968.

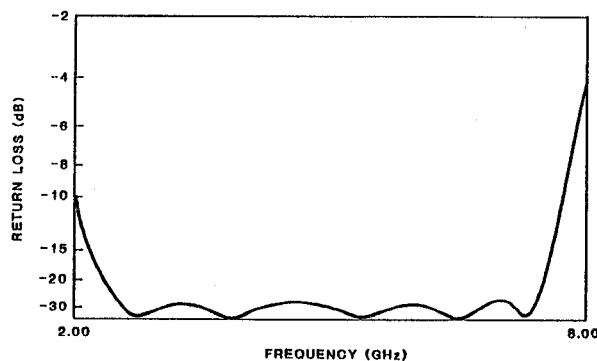
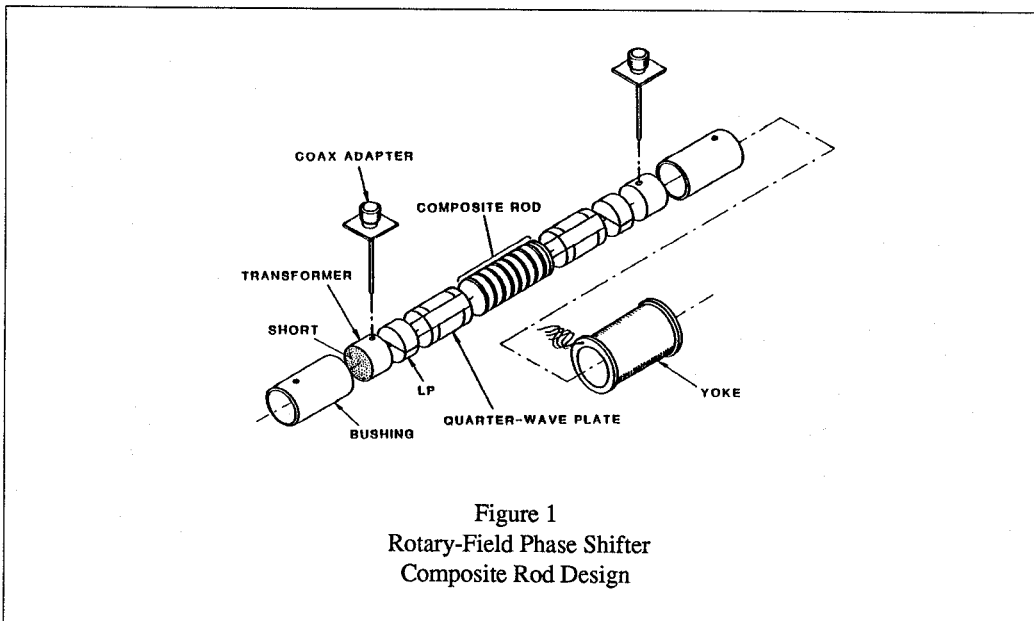


Figure 2
Composite Rod Computed Impedance
Match Characteristic

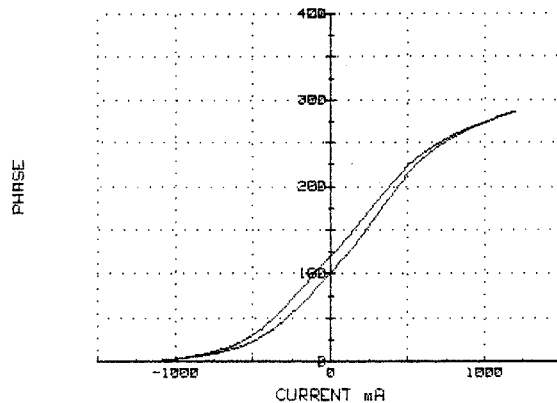


Figure 3
Ferrite Half-wave Plate
Differential Phase Characteristic

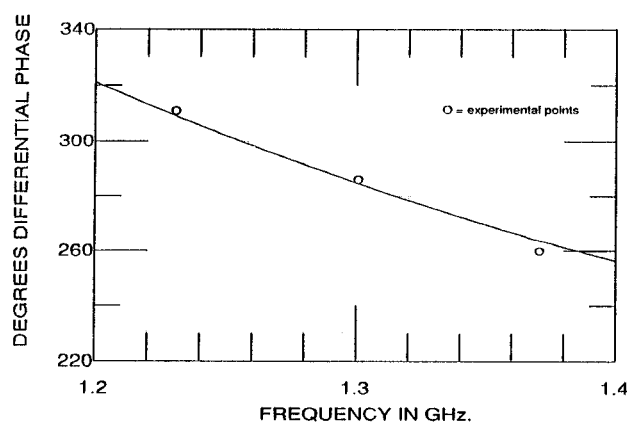


Figure 4
Half-wave Plate
Frequency Dispersion

